Catal Lett (2014) 144:1016–1022
DOI 10.1007/s10562-014-1232-6

Depletion NO_x Made Easy by Nitrogen Doped Graphene

Xilin Zhang · Zhansheng Lu · Yanan Tang · Dongwei Ma · Zongxian Yang

Received: 19 November 2013 / Accepted: 28 February 2014 / Published online: 16 March 2014

Abstract The integrated mechanism of the catalytic oxidation of NO by N_2O on the metal-free support of nitrogen doped graphene (NG) is investigated using density function theory calculations. The results indicate that the N_2O can be intensively adsorbed on NG support, while the NO, N_2, NO_2 are all weakly adsorbed. In the oxidation process, a two-step mechanism is identified: the dissociation of N_2O followed by the oxidation of NO with the dissociative O-atom. The present work suggests that the NG support, as a high-efficient and metal-free catalyst, is one of the promising candidates for removing the nitrogen oxides gases exhaust.

Keywords Metal-free · Nitrogen doped graphene · Depletion NO_x

1 Introduction

The production of poisonous gases from the combustion of fuel, vehicles, and industrial processes is considered to be one of the big environmental issues to be solved. Among the poisonous gases, nitrogen oxides (NO_x) are considered to be the most toxic gases emitted into the atmosphere. For example, the NO, a major atmospheric pollutant, has aroused wide public concern experimentally and theoretically [1–3]. N_2O has been recognized as one of the contributors to global warming and also a cause of ozone depletion [4]. So effective strategy to reduce NO and N_2O is necessary for the protection of the ozone layer and control of global warming effects.

The conventional method used to reduce the NO_x emissions is the selective catalytic reduction (SCR) with ammonia as the reduction agent [5–7]. The SCR processes for denoxing with ammonia as the reduction agent are:

$$4NH_3 + 4NO + O_2 \rightarrow 4N_2 + 6H_2O \quad (1)$$

$$4NH_3 + 6NO \rightarrow 5N_2 + 6H_2O \quad (2)$$

However, the use of ammonia causes additional problems, e.g., the ammonia slip [8], which brings about additional environment problem. In the NO_x depletion process using the metal-free nitrogen doped graphene (NG) catalyst, the poisonous ammonia is not needed. Additionally, the metal-free NG catalyst avoids the high costs of the traditional noble metal catalysts. Another efficient method to deplete NO is the oxidation of NO into NO_2, which is then captured by water [9–12]. Moreover, given the decisive role of the NO_2 in exhaust gas after treatment techniques, efforts made by a number of researchers in the past decade have resulted in a wide number of catalysts for this reaction [2, 13–16].

Because of the damage of N_2O to the environment, as of today, decomposition of the N_2O molecule has been considered to be an efficacious method to remove it [17]. For instance, Zhao et al. [18] found that Rh/ALHT catalyst is stable for decomposition of N_2O, but needs a higher start temperature. Lv et al. [19] revealed that N_2O molecule decomposes easily on Al- and Ga-embedded graphene, but needs an appropriate external electric field.

As mentioned above, the poisonous NO and N_2O are harmful to the environment and difficult to be eliminated.

X. Zhang · Z. Lu (✉) · Y. Tang · Z. Yang (✉)
College of Physics and Electronic Engineering, Henan Normal University, 453007 Xinxiang, China
e-mail: zslu@henannu.edu.cn

Z. Yang
e-mail: yzx@henannu.edu.cn

D. Ma
School of Physics, Anyang Normal University, 455000 Anyang, China

Therefore, finding appropriate low temperature and base metal catalysts, even metal-free catalysts, to accelerate the reactions for the abatement of NO and N_2O has become a key challenge. Recently, Wang and Pantelides [20] suggested that NO can be removed easily with adsorbed O on NG based on first-principles molecular dynamics simulations. Besides, Chen et al. [1] found that NO can be easily converted into N_2O through a dimer mechanism on Si-doped graphene. Zhao et al. [21] illustrated that N_2O decomposition occurs easily on the same support. Although segments about the reaction of NO_x (NO and N_2O) are studied and described, the reaction mechanism is not well addressed. With nitrogen doping in the monolayer graphene, the spin density and charge distribution of carbon atoms will be influenced by the neighbor nitrogen dopant [22, 23], which induce the "activation region" on the graphene surface. This kind of activated region can participate in catalytic reaction directly, such as the oxygen reduction reaction [23, 24]. Whether or not the NG catalyst can catalyze the decomposition of N_2O? Whether or not the NG can eliminate the NO_x simultaneously? Motivated by this, we apply the first-principles calculation to study the adsorption and reaction of the poisonous gases (NO_x) on NG. The reaction mechanism and the integrated reaction process are investigated. Our results demonstrate that NG, a metal-free catalyst, would be a promising candidate for eliminating the toxic NO_x gases and plays an important role in the protection of the environment and resources.

2 Calculation Method and Model

Periodic density function theory calculations are performed using the Vienna Ab-initio Simulation Package (VASP) [25]. For improving the calculation efficiency, core electrons are replaced by the projector augmented wave pseudo-potentials [26] and the generalized gradient approximation of the Perdew, Burke, and Ernzernhof (PBE) functional [27] is used for the exchange and correlation. The wave functions are expanded in plane waves with a cut off energy of 450 eV and the convergence criterion for the electronic self-consistent iteration is set to 10^{-5} eV. The NG layer and the adsorbates are free to relax until the self-consistent force drop to below 0.02 eV $Å^{-1}$. With the purpose of avoiding the interactions due to the artificial periodicity, a vacuum layer of 15 Å is used to separate the periodic images in the direction perpendicular to the surface. The Brillouin zone integration is performed with a $3 \times 3 \times 1$ Γ-centered Monkhorst–Pack (MP) grid. We also make a comparison test with a $5 \times 5 \times 1$ MP grid and find only tiny changes in energy (0.01 eV).

The climbing image nudged elastic band method (CI-NEB) [28–30] is employed to investigate the saddle points and minimum energy paths (MEP). The spring force between adjacent images is set to 5.0 eV $Å^{-1}$. Images are optimized until the forces on each atom drop to below 0.02 eV $Å^{-1}$. The energy barriers are calculated using the initial state (IS) as a reference.

The Bader's "atoms in molecules" theory [31] is used to assign charges to atoms and fragments. These charges provided useful clues to how the charge transfers between different atoms or fragments. One major issue with the normal charge density from the VASP code is that they only contain the valence charge density, which would give an unreal charge transfer of N dopant by Bader charge analysis in the NG systems. Considering this point, the core charge is included for Bader charge analysis in the current study, by which a real charge transfer could be obtained.

The adsorption energy is defined by the formula.

$$E_{ad} = E_{NG} + E_X - E_{(X/NG)} \quad (3)$$

where $E_{(X/NG)}$ and E_{NG} are the spin-polarized total energies for the optimized equilibrium configurations of NG with and without gas adsorbate (X), respectively, and E_x is the spin-polarized total energy of the corresponding isolated gas molecule in its ground state. With this definition, a higher E_{ad} value means a stronger adsorption.

The NG system is modeled using a 6×6 hexagonal graphene supercell with three substitutional nitrogen dopant atoms as shown in Fig. 1 (all figures generated using the VESTA package) [32]. Our previous work [33] has proved that such a NG system has high catalytic activity for oxygen dissociation. Electrochemical tests also indicated that this catalyst had the highest activity for oxygen reduction via a four-electron pathway. Using first-principles calculation method, Feng et al. [34] revealed that nitrogen clusters other than the isolated one are the most efficient catalytic sites for oxygen reduction. In addition, Yang and colleague [35] also pointed out that this kind of nitrogen has a higher catalytic effect for oxygen dissociation than other types, such as pyridine-like nitrogen atoms. Based on these facts, we use the NG model as the substrate in all of our calculations. The calculated lattice constant of pristine graphene (PG) is 2.46 Å, which is consistent with the values of other groups [36–38]. The C–N bond length in the optimized NG is 1.41 Å, which is reduced by 0.1 Å compared with C–C bond length in the PG, 1.42 Å, in agreement with the results of Dai et al. [39].

3 Results and Discussion

3.1 The Adsorption of Toxic Gases on NG

Before exploring the catalytic oxidation of NO by N_2O, we start our study by investigating the geometric structure of

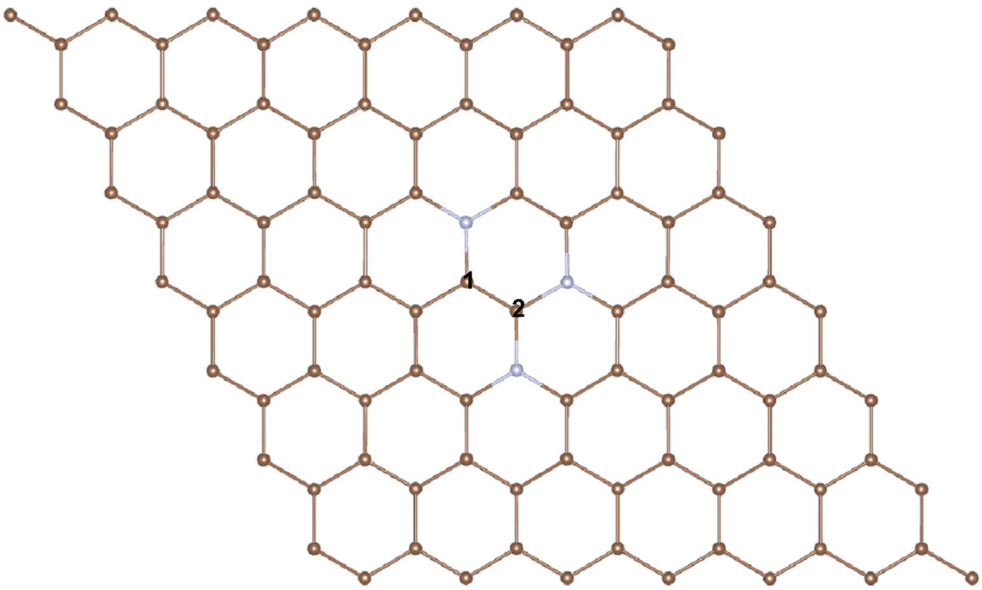

Fig. 1 The top view of the nitrogen doped graphene model. Hereafter, the *brown* and *blue spheres* denote the C and N atoms, respectively

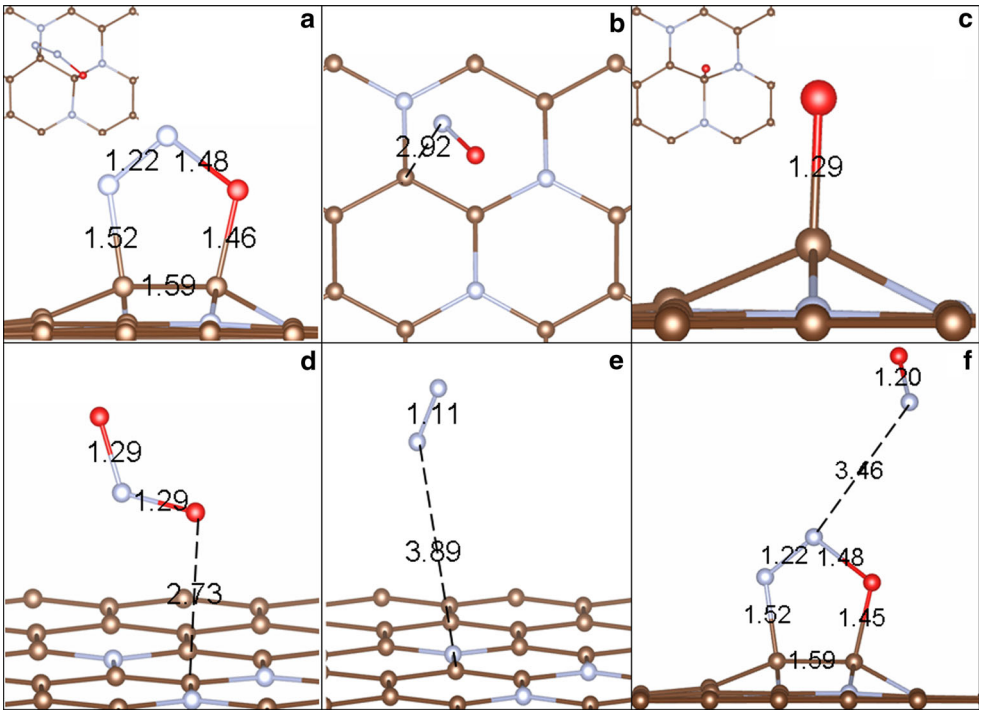

Fig. 2 The most stable configuration of various reaction or intermediate gases adsorbed on the nitrogen doped graphene (NG): **a** N_2O, **b** NO, **c** atomic O, **d** NO_2, **e** N_2, **f** N_2O and NO coadsorption. The *inset* pictures in **a** and **c** are the top views. *Red spheres* denote O atoms

toxic gases adsorption on NG. For each adsorbate, we consider various adsorption sites and different adsorption patterns. In Fig. 2, we depict the most stable configurations for each adsorbate and intermediate products. The corresponding adsorption energies, the shortest distance between adsorbate and support and the bond lengths of the reaction gases before (after) adsorption are list in Table 1. The corresponding quantitative effects of the van-der-Waals (vdW) correction [40] are examined. It is found that the vdW correction becomes important when the adsorption energy is small enough. The adsorption energies increase quite a lot, while the adsorbate-NG distances (d_{nn}) decrease accordingly, indicating that the calculations without the vdW corrections underestimate the strength of the adsorption. However, the adsorption can still be assigned as physisorption, which have relatively small adsorption energies, large adsorbate-NG distances (d_{nn}) and almost unchanged intramolecular distances ($d_{N–N}$ or $d_{N–O}$). In the following, we will mainly present the results without the vdW corrections.

The calculated result indicate that N_2O is intensely adsorbed on NG and the most stable adsorption configuration is that the N- and O-atoms of N_2O bind with the C–C bond

Table 1 Adsorption energy (E_{ad}) of reactants and intermediate products adsorbed on NG, the shortest distance between the adsorbates and NG (d_{nn}), the N–N (d_{N-N}) and/or N–O (d_{N-O}) bond lengths of the reaction gases before (after) adsorption

Adsorbate	E_{ad} (eV)		d_{nn} (Å)		d_{N-N} (Å)		d_{N-O} (Å)	
N_2O	2.67[a]	–	1.46[a]	–	1.15 (1.22)[a]	–	1.23 (1.48)[a]	–
NO	0.23[a]	0.65[b]	2.92[a]	2.37[b]	–	–	1.19 (1.22)[a]	1.20 (1.23)[b]
O	5.06[a]	5.22[b]	1.29[a]	1.29[b]	–	–	–	–
N_2	0.03[a]	0.20[b]	3.89[a]	3.65[b]	1.11 (1.11)[a]	1.11 (1.11)[b]	–	–
NO_2	0.30[a]	0.77[b]	2.73[a]	2.59[b]	–	–	1.28 (1.29)[a]	1.28 (1.30)[b]

The superscripts "a" and "b" represent for the results without and with van-der-Waals correction, respectively

surrounded by three nitrogen atoms and form a five-member ring, which is similar to the N_2O adsorbed on Si-embedded graphene [21]. In this most stable geometry, the adsorbate and the support are all distorted seriously, as shown in Fig. 2a, where the insert picture is a top view. The calculated adsorption energy is 2.67 eV with quite amount of electrons (0.50 e) transferred from NG to N_2O.

The adsorptions of NO and N_2 all can be assigned as physisorption both for the cases with and without the vdW correction. The end-on configuration is favored with the lowest E_{ad} values and large d values as shown in Fig. 2b and e, respectively. The weak physisorption is further verified by the negligible amounts of charge transfer, 0.09 and 0.02 e from NG for NO and N_2 adsorption, respectively. When the vdW force is considered, the adsorption is enhanced with the shortest distances between the adsorbates and NG shortened from 2.92 to 2.37 Å for NO and from 3.89 to 3.65 Å for N_2, while the most stable adsorption configurations remain unchanged.

The atomic O, a kind of intermediate product, can be strongly bound to the top site of the carbon atom that directly connects with the two nitrogen dopant atoms as shown in Fig. 2c, with an E_{ad} of 5.06 eV and the C–O bond length of 1.29 Å. There are 0.80 electrons transferred from NG to O atom, which makes the C–C length elongated from 1.42 to 1.52 Å and the bonded carbon atom dragged by 0.04 Å away from the support surface. This observation indicates that the oxygen atom can strongly pull the charge back from the NG support due to its strong electronegativity and lead to an intense interaction.

The most energetically favorable adsorption configuration of NO_2 is shown in Fig. 2d. The adsorbed NO_2 has a quite large distance (2.73 Å) from the support. The calculated adsorption energy is 0.30 eV accompanied by a charge transfer of 0.60 e from NG to NO_2, which leads to the N–O bond enlarged from 1.28 to 1.29 Å. Upon considering vdW correction, the shortest distance between NO_2 and the NG support is reduced to 2.59 Å and the adsorption energy is increased to 0.77 eV. Similar to NO and N_2, the intramolecular configuration of NO_2 is kept its optimal configuration whatever the vdW correction is considered or not.

3.2 The Oxidation of NO by N_2O on NG

According to the possible situation of two reactant gases (nitrous oxide and nitric oxide) completely mixed, the reaction mechanisms are divided into two pathways depending on the adsorption strength, i.e., the Eley–Rideal (ER) and Langmuir–Hinshelwood (LH) mechanisms. For the ER mechanism, the gas-phase NO molecule approaches and reacts with the already-activated N_2O, while the LH mechanism involves the coadsorption of NO and N_2O molecules before reaction.

Comparing the adsorption properties of NO on NG with that of N_2O, we found that the N_2O molecule is preferred to be attached to the NG support surface than NO. Therefore, when NO and N_2O mixture is injected as the reaction gas, the NG support would be covered by the N_2O molecule. To verify this, we make a test by exploring the coadsorption of NO and N_2O. The most stable coadsorption configuration is exhibited in Fig. 2f, which shows clearly that the activity region of NG are completely occupied by N_2O when NO and N_2O are coadsorbed. The calculated coadsorption energy is 2.73 eV, which is slightly smaller than the sum of the respective adsorption energies of NO and N_2O ($2.67 + 0.25 = 2.92$ eV) on NG, indicating that the cooperative adsorption of NO and N_2O is weak. Our simulation results show that the shortest distance between NO and N_2O is 3.45 Å, which is in line with the weak coadsorption effect. In short, all the results indicate that there is only a quite weak interaction between NO and N_2O.

On the basis of these results, we conclude that it is quite hard for the NO and N_2O reaction to occur on NG along the LH mechanism. So, we turn our attention to the ER mechanism.

The reaction mechanism is proposed to occur in stepwise reactions, i.e., the decomposition of N_2O followed by the oxidation of NO as presented in formulas (4) and (5).

The adsorption and decomposition of N_2O:

$$N_2O + NG \rightarrow N_2 + O^* + NG \quad (4)$$

The adsorption and oxidation of NO:

$$NO + O^* + NG \rightarrow NO_2 + NG \quad (5)$$

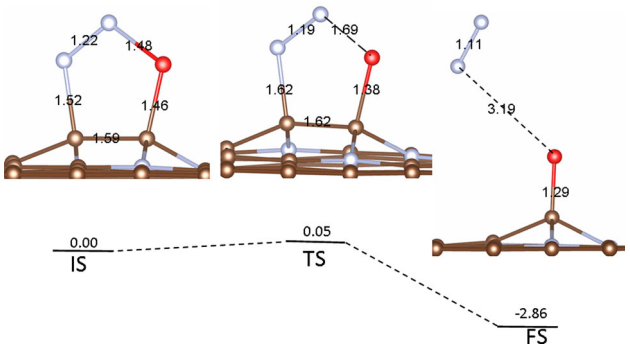

Fig. 3 The MEP for the decomposition of the N_2O on NG. All energies are reported in eV relative to the initial state and the distances are in angstrom

Firstly, we discuss the N_2O decomposition on NG. To search for the MEP for this reaction, we selected the configuration shown in Fig. 2a as the IS. The final state (FS) is that a N_2 molecule physically adsorbed on NG with a chemisorbed atomic O at the top site of carbon atom. The corresponding MEP profile is summarized in Fig. 3. The energetic is schematically plotted with respect to the reference energy of the IS. The local configurations of the adsorbate on NG at various states along the MEP are also displayed in Fig. 3, which shows that the N–O and N–C bonds are elongated from 1.48 and 1.52 Å in the IS to 1.69 and 1.62 Å in the transition state (TS), respectively, with a rather small energy barrier of 0.05 eV along the reaction pathway. The C–C bond connected to the N_2O in the substrate is also elongated (from 1.59 to 1.62 Å). In contrast, the N–N and C–O bonds are shrunk from 1.22 and 1.46 Å to 1.19 and 1.38 Å, respectively. Finally, the C–N–N–O–C five-member ring is broken, resulting in the formation of a N_2 molecule and an atomic O adsorbed on the C atom (denoted as O/NG, the NG with atomic O adsorbate) as shown in the FS.

Due to the weak interaction between the N_2 molecule and the O/NG ($E_{ad} = 0.03$ eV), the N_2 molecule can be easily desorbed. The energy released in the dissociation of N_2O on NG is 2.86 eV. In light of the small barrier (0.05 eV) and large exothermicity (2.86 eV), it is expected that the dissociation of N_2O can be achieved easily on the metal-free NG support.

The decomposition process of N_2O found in this paper is similar to that on the Si-embedded graphene [21], but different from that on the Fe-embedded graphene [41], which indicated that the decomposition barriers of N_2O on Si-embedded graphene and Fe-embedded graphene is about 0.02 and 0.35 eV, respectively. Our calculated barrier (0.05 eV) is comparable with that on the Si-embedded graphene (0.02 eV) and much smaller than those on the transition metals [17], e.g., Fe (41 kJ mol^{-1}), Co (28 kJ mol^{-1}) and Rh (35 kJ mol^{-1}). More importantly, the NG support is metal-free. In addition, compared with the Rh/ALHT catalyst [18], the NG could work at low temperature and does not need external electric field [19]. It is therefore expected that the NG is an excellent metal-free catalyst for the abatement of N_2O.

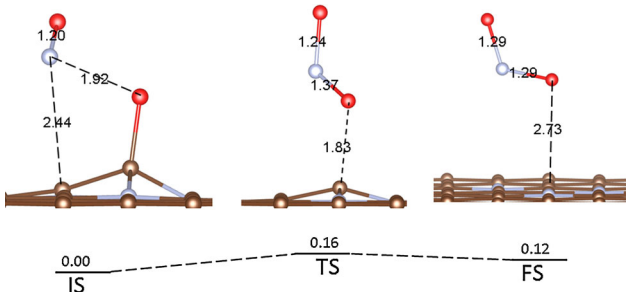

Fig. 4 The MEP for the NO oxidation by the dissociative O

Since an atomic O is left on the NG support in the process of N_2O dissociation, it is necessary to explore whether this atomic O can be further reduced by subsequent NO molecules via ER mechanism. It is expected that the NO molecule can be oxidized easily by the O/NG intermediate due to the strong negative charge on the O atom, which can attract the N atom of the NO. This has been verified by Wang and Pantelides [20].

The adsorption and oxidation of NO on the O/NG are studied. The process is depicted in Fig. 4, where a NO is initially adsorbed with a configuration as shown Fig. 4a (IS) and the FS is set as the configuration with NO_2 adsorbed on the NG (as shown Fig. 2d). The simulation results indicate that the N-atom of NO first approaches the adsorbed O-atom and reaches the TS. The distance between NO and the O atom is shortened from 1.92 Å of IS to 1.37 Å of TS in this endothermic process. At the same time, a NO_2-like molecule is formed and sits at the height of 1.83 Å above the NG. The transition barrier is 0.16 eV. Passing over the TS, a NO_2 molecule is formed and desorbed, leading to the recovery of the NG. Once formed, the NO_2 can be collected easily by water [9–12], resulting in the useful product, such as H_2NO_3. Our calculated barrier for NO oxidation on NG (0.16 eV) is much smaller than the result of Schneider et al. [15] for the NO oxidation on Pt(111) (1.28 eV), indicating that the NO oxidation is more moderate on the metal-free NG catalyst than on the noble metal Pt. Additionally, Oliver et al. [2] pointed out that NO_2 as the product of NO oxidation on Pt/SiO_2 inhibits the further oxidation of NO. They also suspected that this catalyst would be deactivated because the formation of platinum oxide on the surface of the platinum particles. In contrast, the NG catalyst proposed here can conquer these obstacles completely.

The influence of vdW correction on the barrier energies is also considered. It is found that on the one hand, when

the vdW correction is considered, the interaction between N_2O and the NG support is enhanced and the barrier of the N_2O decomposition is changed to almost 0.00 eV, corresponding to the spontaneous decomposition of N_2O, which is in agreement with the case for the results of the N_2O decomposition (with a barrier of 0.05 eV) without the vdW correction.

On the other hand, when the vdW correction is considered, the NO oxidation process is the same and the geometric configuration is almost unchanged compared with the result without including the vdW correction, but the barrier increases to 0.26 from 0.16 eV.

In conclusion, the results testify again that the NG support is a high-efficient metal-free catalyst for the catalytic oxidation of NO by N_2O.

It should be pointed out that, in the catalysis theory, the overall barrier is important rather than a particular barrier. Usually, if one of the intermediate reactions is endothermic, the overall barrier can be higher than all the particular ones. Then, the overall barrier should be equal to the highest particular one [21, 42]. For the stepwise oxidation process of NO by N_2O on NG, the oxidation of NO by O adatom on NG is the rate-limiting step with a small barrier of 0.26 eV. The results indicate that the NG as a metal-free catalyst exhibits high catalytic activity for NO oxidation by N_2O, and may be a promising candidate as a substitute for noble metal catalyst.

The high reaction activity of NG toward the NO catalytic oxidation by N_2O can be further understood according to the Bader charge analysis. The results are shown in Table 2, which shows that the C_1 and C_2 atoms in the center of the N dopant cluster lose about 0.47 and 0.68 electrons, respectively. The carbon dimer, which loses 1.15 e in total, is just the most preferred adsorption site and the active center for the catalytic oxidation of NO by N_2O. Compared with the pure the NG support, the C-dimer further loses electrons (1.45–1.69 vs 1.15) with the adsorption of N_2O and O, respectively. The same phenomenon was observed when the NO, N_2 and NO_2 were adsorbed on the NG support as shown in Table 2, indicating that the electrons transferred from the NG support to the adsorbates are mainly from the carbon dimer. For example, upon the cleavage of the N–O bond of the N_2O on the NG support (Fig. 3), the C-dimer loses about additional 0.53 electrons. Compared the situation of O adsorption with that of N_2 and O coadsorption, the same amount of charge transfer is found at the C-dimer, indicating that the N_2 molecule has almost no interaction with the NG support, which is in line with the weak adsorption as mentioned above. We also find that in this process the effect of C_2 atom is more important than the C_1 atom because of the more charge transfer of the C_2 atom. The same effect is observed in the process of NO oxidation by O atom.

Table 2 The results of Bader charge analysis (in *e*)

adsorbate	q(adsorbate)	q(C_1)	q(C_2)	q(C-dimer)
pure	–	−0.47	−0.68	−1.15
N_2O	0.50	−0.34	−1.11	−1.45
N_2	0.02	−0.40	−0.85	−1.25
O	0.80	−0.39	−1.30	−1.69
NO_2	0.60	−0.36	−1.00	−1.36
NO	0.09	−0.43	−1.00	−1.43
O+NO	0.68	−0.45	−1.18	−1.63
N_2+O	0.55	−0.38	−1.30	−1.68

q(adsorbate) stands for the total charge on the adsorbate. q(C_1) and q(C_2) represent the charge of the C_1 and C_2 atoms as labeled in the Fig. 1 and the q(C-dimer) represent the total charge of C_1 and C_2. The positive and negative numbers represent the electrons accumulation and depletion, respectively

According to the results above, the process of the NO_x depletion process on NG could be summarized as $N_2O + NO \rightarrow N_2 + NO_2$, and the best content of NO and N_2O for the NO depletion on NG is 1:1 (mole ratio). If the content of NO is higher than N_2O, in order to remove NO sufficiently, additional oxygen molecule would be needed. Fortunately, the dissociation of O_2 is very moderate on NG as mentioned above [23, 24, 33, 35]. So, when N_2O is scanty, the O_2 could be used as oxidant. In this case, the best mole ratio of NO, N_2O and O_2 is 4:2:1. This can be summarized as $4NO + 2N_2O + O_2 \rightarrow 2N_2 + 4NO_2$.

It is worth noting that the content of N_2O is smaller than NO in exhaust gases practically. When O_2 is insufficient, the N_2O could be dissociated completely; but the NO may be spillover. However, if the content of O_2 is enriched or is comparable with N_2O, the NO could be removed completely; but it may result in a competition reaction and N_2O spillover. Keeping this in mind, future experimental studies are greatly desired to probe the optical ratio of N_2O and O_2.

4 Conclusion

The adsorption and reaction properties of NO_x on NG are discussed. The reaction mechanism and the minimum energy path are addressed. It is found that the N_2O molecule can be strongly adsorbed on the NG, while the NO, N_2 and NO_2 can only be weakly adsorbed. When the vdW correction is considered, the adsorption energies are enhanced by about 0.4 eV with the adsorbate-NG distances shortened for NO, N_2 and NO_2. However, the adsorption configurations almost remain unchanged. The minimum energetic reaction path is evaluated. The results show that the N_2O adsorbed on NG can be decomposed easily into atomic O and N_2 with a barrier of 0.05 eV. Then the adsorbed NO molecule can be oxidized readily by the

atomic O with a barrier of 0.16 eV. The present work suggests that NG is an efficient metal-free catalyst for NO catalytic oxidation by N_2O and is one of the promising candidates for solving the environmentally harmful exhaust NO_x from vehicles and industrial wastes.

Acknowledgments This work is supported by the National Natural Science Foundation of China (Grant No. 11174070 and 11147006). Z. Lu also acknowledges the support from the China Postdoctoral Science Foundation funded project (Grant No. 2012M521399) and Postdoctoral Research sponsorship in Henan Province (Grant No. 2011038), Foundation for the Key Young Teachers of Henan Normal University and Start-up Foundation for Doctors of Henan Normal University. Parts of the simulations are performed on resources provided by the high-performance computing center of College of Physics and Electronic Engineering in Henan Normal University.

References

1. Chen Y, Liu Y-J, Wang H-X, Zhao J-X, Cai Q, Wang X-Z, Ding Y (2013) ACS Appl Mater Interfaces 5:5994
2. Després J, Elsener M, Koebel M, Kröcher O, Schnyder B, Wokaun A (2004) Appl Catal B 50:73
3. Parvulescu V, Grange P, Delmon B (1998) Catal Today 46:233
4. Ravishankara A, Daniel JS, Portmann RW (2009) Science 326:123
5. Qi G, Yang RT (2003) Appl Catal B 44:217
6. Qi G, Yang RT, Chang R (2004) Appl Catal B 51:93
7. Topsoe N, Topsoe H, Dumesic J (1995) J Catal 151:226
8. Koebel M, Elsener M, Kleemann M (2000) Catal Today 59:335
9. Bambauer A, Brantner B, Paige M, Novakov T (1994) Atmos Environ 28:3225
10. Chan WH, Nordstrom RJ, Calvert JG, Shaw JH (1976) Sci Technol 10:674
11. Mochida I, Kawabuchi Y, Kawano S, Matsumura Y, Yoshikawa M (1997) Fuel 76:543
12. Philips DA, Dasgupta PK (1987) Sep Sci Technol 22:1255
13. Ovesson S, Lundqvist B, Schneider W, Bogicevic A (2005) Phys Rev B 71:115406
14. Sousa JP, Pereira MF, Figueiredo JL (2011) Catal Today 176:383
15. Xu Q-Q, Yang H-Q, Gao C, Hu C-W (2013) Struct Chem 24:13
16. Yang H, Liu H, Zhou K, Yan Z-Q, Zhao R, Liu Z-H, Liu Z-H, Qiu J-R (2012) J Fuel Chem Technol 40:1002
17. Yakovlev AL, Zhidomirov GM, van Santen RA (2001) Catal Lett 75:45
18. Zhao X, Cong Y, Lv F, Li L, Wang X, Zhang T (2010) Chem Commun 46:3028
19. Lv Y-A, Zhuang G-L, Wang J-G, Jia Y-B, Xie Q (2011) Phys Chem Chem Phys 13:12472
20. Wang B, Pantelides S (2011) Phys Rev B 83:245403
21. Zhao J-X, Chen Y, Fu H-G (2012) Theor Chem Acc 131:1
22. Groves M, Chan A, Malardier-Jugroot C, Jugroot M (2009) Chem Phys Lett 481:214
23. Zhang L, Xia Z (2011) J Phys Chem C 115:11170
24. Shao Y, Zhang S, Engelhard MH, Li G, Shao G, Wang Y, Liu J, Aksay IA, Lin Y (2010) J Mater Chem 20:7491
25. Kresse G, Furthmüller J (1996) Comput Mater Sci 6:15
26. Kresse G, Joubert D (1999) Phys Rev B 59:1758
27. Perdew JP, Burke K, Ernzerhof M (1996) Phys Rev Lett 77:3865
28. Henkelman G, Jónsson H (2000) J Chem Phys 113:9978
29. Henkelman G, Uberuaga BP, Jónsson H (2000) J Chem Phys 113:9901
30. Zhu T, Li J, Yip S (2004) Phys Rev Lett 93:025503
31. Kocher N, Henn J, Gostevskii B, Kost D, Kalikhman I, Engels B, Stalke D (2004) J Am Chem Soc 126:5563
32. Momma K, Izumi F (2008) J Appl Crystallogr 41:653
33. Chao S, Lu Z, Bai Z, Cui Q, Qiao J, Yang Z, Yang L (2013) Int J Electrochem Sci 8:8786
34. Feng Y, Li F, Hu Z, Luo X, Zhang L, Zhou X-F, Wang H-T, Xu J-J, Wang E (2012) Phys Rev B 85:155454
35. Ni S, Li Z, Yang J (2012) Nanoscale 4:1184
36. Girit ÇÖ, Meyer JC, Erni R, Rossell MD, Kisielowski C, Yang L, Park C-H, Crommie M, Cohen ML, Louie SG (2009) Science 323:1705
37. Pedersen TG, Flindt C, Pedersen J, Mortensen NA, Jauho A-P, Pedersen K (2008) Phys Rev Lett 100:136804
38. Reich S, Maultzsch J, Thomsen C, Ordejon P (2002) Phys Rev B 66:035412
39. Dai J, Yuan J, Giannozzi P (2009) Appl Phys Lett 95:232105
40. Klimeš J, Bowler R, Michaelides A (2011) Phys Rev B 83:195131
41. Wannakao S, Nongnual T, Khongpracha P, Maihom T, Limtrakul J (2012) J Phys Chem C 116:16992
42. Song E, Wen Z, Jiang Q (2011) J Phys Chem C 115:3678